

Article

The Fabrication of a UV Notch Filter by Using Solid State Diffusion

Hung-Pin Chen ^{1,2,*} , Wen-Hao Cho ^{1,*}, Wei-Chun Chen ¹, Chao-Te Lee ¹ and Cheng-Chung Lee ²

¹ National Applied Research Laboratories, Taiwan Instrument Research Institute, Hsinchu 30076, Taiwan; weichun@itrc.narl.org.tw (W.-C.C.); tigerlee@itrc.narl.org.tw (C.-T.L.)

² Department of Optics and Photonics, National Central University, Chungli 32001, Taiwan; clee@dop.ncu.edu.tw

* Correspondence: chbin@itrc.narl.org.tw (H.-P.C.); kesikar@itrc.narl.org.tw (W.-H.C.); Tel.: +886-3-577-9911 (H.-P.C.)

Received: 26 February 2019; Accepted: 20 March 2019; Published: 23 March 2019



Abstract: One of the methods used to obtain notch filters involves one or several gradient index layers. In this method, the indices are decreased and then increased step by step to create a sinusoidal-like gradient layer. This paper reports a sinusoidal-like gradient layer fabrication method based on solid state diffusion. $\text{Al}_2\text{O}_3/\text{MgO}/\text{Al}_2\text{O}_3$ (AMA) was deposited by electron beam evaporation and then post-annealed at 800 °C for 4 h. Through inner diffusion, the MgO layers became a low refractive index material with a porous structure (the average refractive index was 1.55) such that the MgAl_2O_4 spinel was formed as an inhomogeneous layer with an average refractive index of 1.69. This allowed simply using a structured multilayer, $(\text{Al}_2\text{O}_3/\text{MgO})^8 \text{Al}_2\text{O}_3$, and post-annealing to form a sinusoidal-like gradient layer for a UV notch filter.

Keywords: notch filter; solid state diffusion; sinusoidal-like gradient layer

1. Introduction

Optical coatings with a combination of high and low refractive indices have attracted a significant amount of attention for their applications in distributed Bragg reflectors, notch filters, polarizers, antireflection coatings, and band-pass filters, among others. These optical coatings have excellent performance for optical system design if the refractive indices of each layer are appropriate. To make a layer with the correct refractive index, manufacturers have used co-evaporation [1], co-sputtering [2], adjusting the reactive gas [3], or depositing at an oblique angle [4]. In this study, the Kirkendall effect was applied to obtain a layer with an appropriate refractive.

The Kirkendall effect is a solid-state diffusion phenomenon in metallurgy. In 1942, the first experiment studying this phenomenon was performed by Kirkendall. This effect refers to a non-reciprocal mutual solid-state diffusion process by an interface between two metals, so that vacancy diffusion occurs to compensate for the inequality of the material flow. In a previous study, the modification of the $\text{Al}_2\text{O}_3/\text{ZnO}$ refractive index has been investigated [5,6].

Notch filter describes a structure exhibiting a regular cyclic variation of refractive index resembling a sine or cosine wave. Such structures have the property of reflecting a narrow spectral region and transmitting all others. However, the manufacturing of notch filters is a difficult task. No material can be produced to a varying continuously refractive index; it is usually a trapezoidal discontinuous change. Conversely, an inhomogeneous layer can be deposited that exhibits a variation of refractive index by the co-evaporation method [7,8].

In this study, we found that the Kirkendall effect also occurs at the interface between Al_2O_3 and MgO. Mg atoms diffused into the Al_2O_3 layer and combined with the Al_2O_3 molecules to form the spine of the MgAl_2O_4 structures under specific annealing processes [9]. The effective refractive index of the MgO was decreased by the Kirkendall voids generated in the MgO layer. Figure 1 schematically shows the Kirkendall effect at the interface between MgO and Al_2O_3 [10]. The refractive index of MgO, with generated Kirkendall voids, was 1.55, while that of MgAl_2O_4 was 1.69. The differences in the indices between the layers were small. Owing to the inhomogeneity at the interface of MgO with void/ MgAl_2O_4 and the small difference of the refractive indices of MgO with void and MgAl_2O_4 in comparison with that of MgO and Al_2O_3 , it was possible to construct a notch filter based on $\text{Al}_2\text{O}_3/\text{MgO}/\text{Al}_2\text{O}_3$ multilayer deposition processes. The multilayer structure, $(\text{Al}_2\text{O}_3/\text{MgO})^8 \text{Al}_2\text{O}_3$, then behaved as a sinusoidal-like gradient layer ($\text{MgAl}_2\text{O}_4/\text{MgO}$ with void/ MgAl_2O_4)⁸ after post-annealing, and demonstrated its notch filter application potential [11,12].

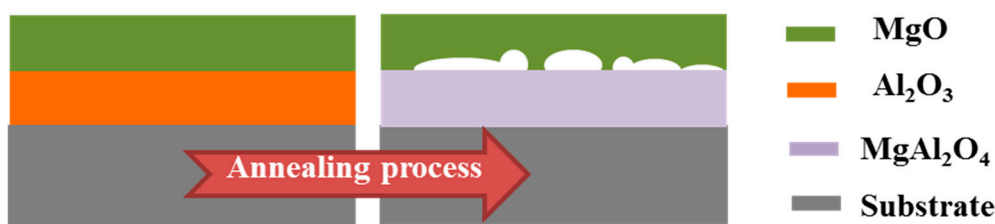


Figure 1. The synopsis illustrations of the Kirkendall effect at the interface of MgO and Al_2O_3 .

2. Experimental

To form a spinel structure for the proposed design, we used Al_2O_3 and MgO. $\text{Al}_2\text{O}_3/\text{MgO}/\text{Al}_2\text{O}_3$ deposited on the quartz substrate using e-gun evaporation with ion-assisted deposition at 300 °C, gun power at 8 KV, and Ar flow rate at 13 sccm. The thicknesses of the layers measured by ellipsometry were 41, 38, and 40 nm respectively. A post-annealing process was implemented without additional gas injection, at 800 °C for 4 h at 1 atm. Inter-diffusions occurred during the post-annealing process through solid state diffusion. Therefore, the refractive indices of the layers changed by the Kirkendall effect. We also performed the deposition and post-annealing process of $(\text{Al}_2\text{O}_3/\text{MgO})^8 \text{Al}_2\text{O}_3$ multilayer as a reflection filter. The optical properties of the multilayer films were measured by a PerkinElmer Lambda 900 spectrometer (Waltham, MA, USA) prepared with an integrating sphere. The cross-sectional microstructures were inspected using a transmission electron microscopy (TEM) and scanning electron microscope (SEM). The composition depth profile of the three-layer structure was inspected by energy dispersive spectroscopy (EDS) line scan analysis and ellipsometry measurement [13]. After the annealing process, the effective refractive indices of the composite films were calculated using the Bruggeman effective medium approximation.

3. Results and Discussions

In Figure 2a, the cross-sectional SEM image of MgO/ Al_2O_3 after annealing at 800 °C shows that, after the annealing process, the voids appeared at the interface of MgO/ Al_2O_3 . It is inferred that complete inter-diffusion reactions between the Al_2O_3 and MgO layers were achieved. The dimension of voids was about 10–20 nm, according to the TEM image in Figure 2b. After the annealing process, the total thickness of the multi-film structure did not change significantly. Figure 3 shows the XRD of Al_2O_3 , MgO, and AMA thin films after a 4-h annealing process at 800 °C. The green line shows the MgO single layer and the blue line shows the Al_2O_3 single layer after a 4-h annealing process at 800 °C. Compared with the red line and black line, the AMA thin-film as deposited (black line) shows non-crystalline MgAl_2O_4 , and the AMA thin-film processes further show the crystalline structure of MgAl_2O_4 , as labeled by the diamond mark.

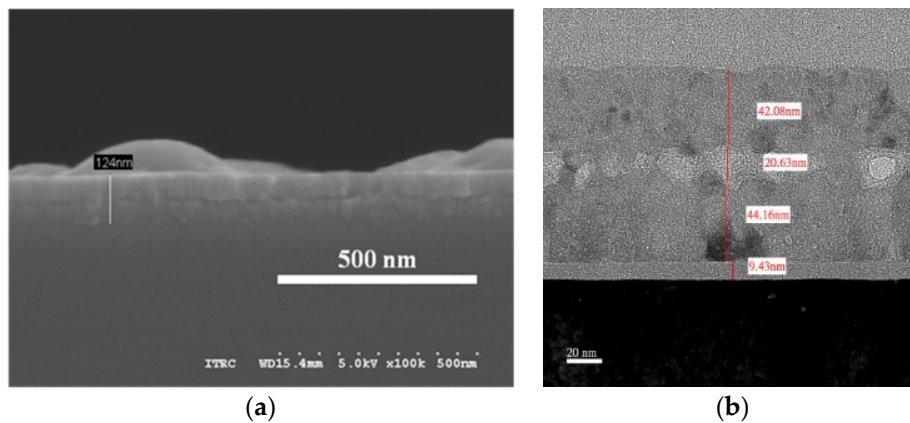


Figure 2. Cross-sectional images of $\text{Al}_2\text{O}_3/\text{MgO}/\text{Al}_2\text{O}_3$ thin films after a 4-h annealing process at 800°C : (a) SEM; and (b) TEM.

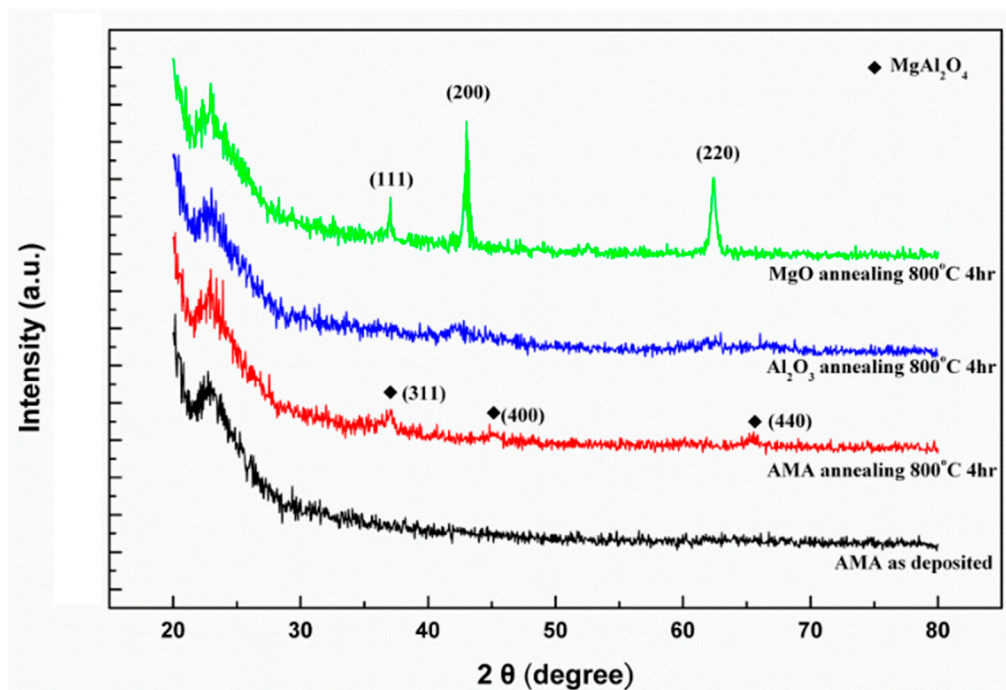


Figure 3. The XRD of Al_2O_3 , MgO , and $\text{Al}_2\text{O}_3/\text{MgO}/\text{Al}_2\text{O}_3$ thin films after a 4-h annealing process at 800°C .

Figure 4 shows the inhomogeneous index profile of $\text{MgAl}_2\text{O}_4/\text{MgO}$ with void/ MgAl_2O_4 when AMA was annealed at 800°C for 4 h, as simulated by the ellipsometry measurement. It started with MgAl_2O_4 moving onto the middle layer MgO with voids, and ended with MgAl_2O_4 . The middle layer was set by MgO , and voids were set with a Gaussian distribution. The middle layer (MgO with voids) exhibited an average porosity of 19.73% by the ellipsometry measurement [14]. The composition depth profile analysis of $\text{MgAl}_2\text{O}_4/\text{MgO}$ with voids/ MgAl_2O_4 by TEM EDS line scan analysis was illustrated by the inter-diffusion mechanism between Al_2O_3 and MgO , as shown in Figure 5. The atomic ratio of Al and Mg were found to be constant in both the top and bottom layers. Additionally, we deposited the $(\text{Al}_2\text{O}_3/\text{MgO})^8 \text{Al}_2\text{O}_3$ multilayer stack and performed the post-annealing process at 800°C for 4 h. After the post-annealing process, the multilayer stack changed from $(\text{Al}_2\text{O}_3/\text{MgO})^8 \text{Al}_2\text{O}_3$ to $(\text{MgAl}_2\text{O}_4/\text{MgO}$ with voids/ $\text{MgAl}_2\text{O}_4)^8$. Figure 6 show the transmittance spectrum as deposited (black line) and after annealing (red line). There was no reflection band in the transmittance spectrum before the post-annealing process. The blue spectrum line in Figure 6 is the transmittance of $(\text{MgAl}_2\text{O}_4/\text{MgO}$ with voids/ $\text{MgAl}_2\text{O}_4)^8$ simulated with a 0.14 refractive index difference between

MgAl₂O₄ and MgO (with voids) at a wavelength of 300 nm. The transmittance spectrum of the multilayer stack after annealing (red line) was close to the simulated result (blue line). This shows that thin film fabrications of (Al₂O₃/MgO)⁸ Al₂O₃ multilayers can be applied as notch filters through solid state diffusion. Solid state diffusion can make the diffusion index difference more gradual in a multilayer structure, which is advantageous in fabricating rugate filters [15,16].

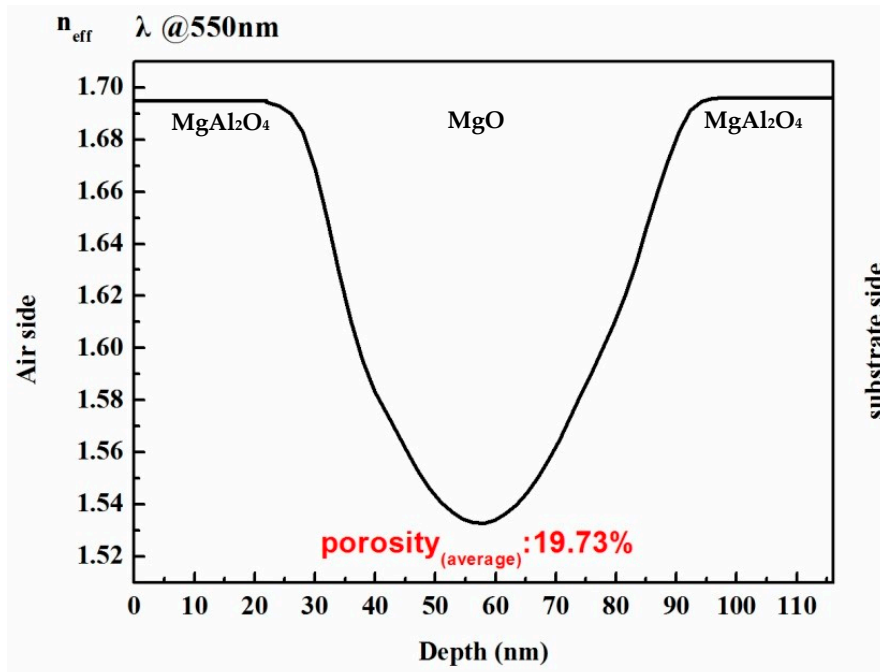


Figure 4. The inhomogeneous index profile of MgAl₂O₄/MgO with void/MgAl₂O₄.

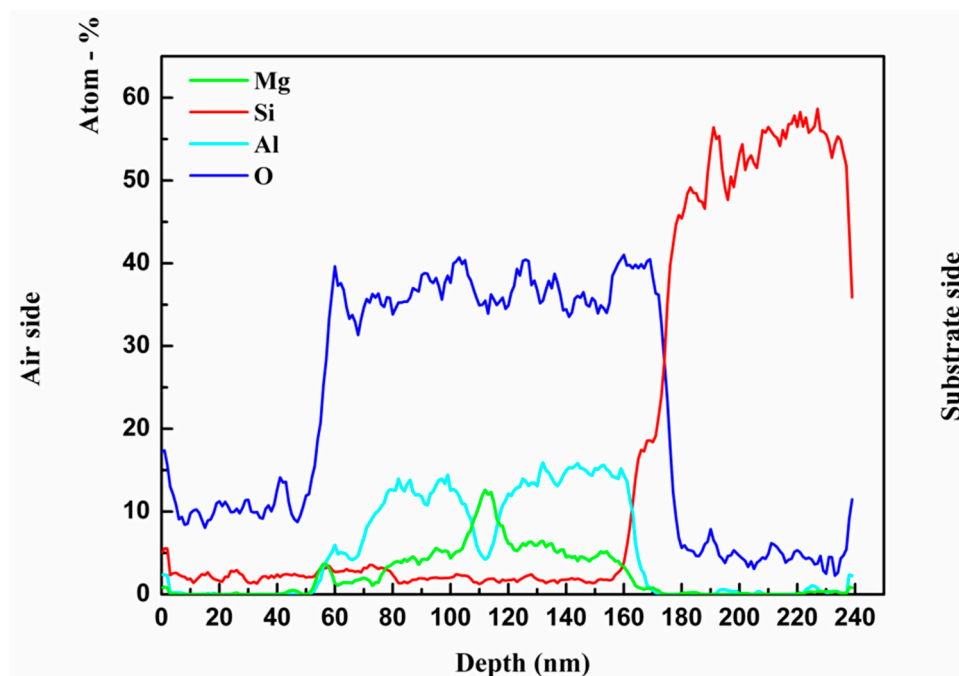


Figure 5. TEM EDS line scan of MgAl₂O₄/MgO with voids/MgAl₂O₄.

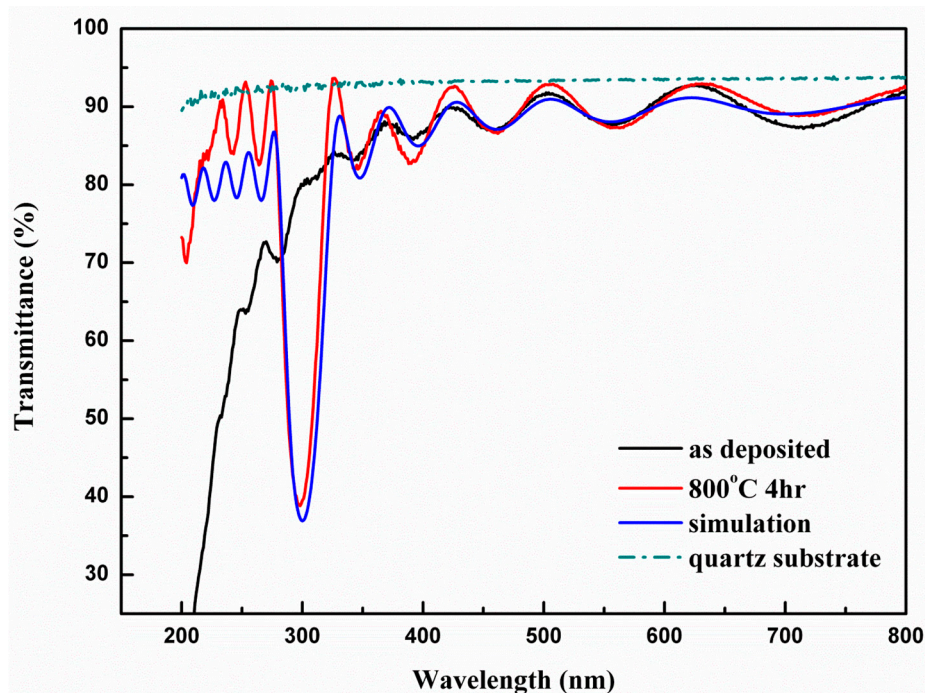


Figure 6. The transmittance spectra of thin films as deposited (black line), after annealing (red line), and according to simulation (blue line).

4. Conclusions

In this study, MgAl_2O_4 and porous MgO layer were successfully fabricated as an AMA structure. The average porosity of MgO with voids was 19.73%, and the refractive index difference between the high (MgAl_2O_4) and low (MgO with voids) index materials was increased to 0.14 by an 800 °C post-annealing process due to solid-state diffusion. This allowed simply using a structured multilayer, $(\text{Al}_2\text{O}_3/\text{MgO})^8 \text{Al}_2\text{O}_3$, and post-annealing to form a sinusoidal-like gradient layer for a UV notch filter. The possibility of solid-state diffusion in multilayer films was demonstrated and a notch filter with a $(\text{MgAl}_2\text{O}_4/\text{MgO with voids}/\text{MgAl}_2\text{O}_4)^8$ multilayer structure was successfully fabricated.

Author Contributions: Conceptualization, H.-P.C. and C.-C.L.; Methodology, H.-P.C. and W.-H.C.; Validation, W.-H.C.; Formal Analysis, W.-C.C. and C.-T.L.; Investigation, W.-H.C.; Data Curation, W.-H.C.; Writing-Original Draft Preparation, H.-P.C. and W.-H.C.; Writing-Review & Editing, H.-P.C. and C.-C.L.

Funding: This research was funded by the Ministry of Science and Technology (Nos. MOST 106-2622-E-492 -017 -CC3 and MOST 107-2622-E-492 -020 -CC3).

Conflicts of Interest: The authors declare that they have no conflict of interest.

References

1. Lee, C.C.; Hsu, J.C. Technique for Deposition Multiplayer Interference Thin films Using Silicon as the Only Coating Material. US Patent 6425978B1, 30 July 2002.
2. Lee, C.C.; Tang, C.J.; Hsu, J.C.; Wu, J.Y. Rugate filter made with composite thin film by ion beam sputtering. *Appl. Opt.* **2006**, *45*, 1333–1337. [[CrossRef](#)] [[PubMed](#)]
3. Lee, C.C.; Hsu, J., C. Technique for Deposition of Multiplayer Interference Thin Film Using Only One Coating Material. ROC Patent Invention No. 137551, 23 June 2001.
4. Hodgkinson, I.; Wu, Q.H.; Brett, M.; Robbie, K. Vacuum deposition of biaxial film with surface-aligned principal axes and large birefringence Δn . *Opt. Soc. Am. Tech. Digest* **1998**, *9*, 104–106.
5. Cho, W.H.; Lee, C.C. Low-refractive-index oxide thin films originated from the Kirkendall effect. *Appl. Opt.* **2014**, *53*, A175–A178. [[CrossRef](#)] [[PubMed](#)]

6. Xi, J.-Q.; Schubert, M.F.; Kim, J.K.; Schubert, E.F.; Chen, M.; Lin, S.-Y.; Liu, W.; Smart, J.A. Optical thin-film materials with low refractive index for broadband elimination of Fresnel reflection. *Nat. Photonics* **2007**, *1*, 176–179. [[CrossRef](#)]
7. Chen, J.; Wang, B.; Yang, Y.; Shi, Y.; Xu, G.; Cui, P. Porous anodic alumina with low refractive index for broadband graded-index antireflection coatings. *Appl. Opt.* **2012**, *51*, 6839. [[CrossRef](#)] [[PubMed](#)]
8. Van Dal, M.J.H.; Gusak, A.M.; Cserháti, C.; Kodentsov, A.A.; van Loo, F.J.J. Microstructural stability of the Kirkendall plane in solid state diffusion. *Phys. Rev. Lett.* **2001**, *86*, 3352. [[CrossRef](#)] [[PubMed](#)]
9. Schubert, E.F.; Kim, J.K.; Xi, J.Q. Low-refractive-index materials: A new class of optical thin-film materials. *Phys. Status Solidi (B)* **2007**, *244*, 3002–3008. [[CrossRef](#)]
10. Kuo, Y. Etch mechanism in the low refractive index silicon nitride plasma enhanced chemical vapor deposition process. *Appl. Phys. Lett.* **1993**, *63*, 144–146. [[CrossRef](#)]
11. Carter, R.E. Mechanism of Solid-state Reaction Between Magnesium Oxide and Aluminum Oxide and Between Magnesium Oxide and Ferric Oxide. *J. Am. Ceram. Soc.* **1961**, *44*, 116–120. [[CrossRef](#)]
12. Rao, C.N.R.; Gopalakrishnan, J. *New Directions in Solid State Chemistry*; Cambridge University Press: Cambridge, UK, 1997; pp. 488–490.
13. Wicht, G.; Ferrini, R.; Schüttel, S.; Zuppiroli, L. Nanoporous Films with Low Refractive Index for Large-Surface Broad-Band Anti-Reflection Coatings. *Macromol. Mater. Eng.* **2010**, *295*, 628–636. [[CrossRef](#)]
14. Redel, E.; Mirtchev, P.; Huai, C.; Petrov, S.; Ozin, G.A. Nanoparticle Films and Photonic Crystal Multilayers from Colloidally Stable, Size-Controllable Zinc and Iron Oxide Nanoparticles. *ACS Nano* **2011**, *5*, 2861–2869. [[CrossRef](#)] [[PubMed](#)]
15. Garcia-Garcia, F.J.; Gil-Rostra, J.; Terriza, A.; González, J.C.; Cotrino, J.; Frutos, F.; Ferrer, F.J.; González-Elipe, A.R.; Yubero, F. Low refractive index SiOF thin films prepared by reactive magnetron sputtering. *Thin Solid Films* **2013**, *542*, 332–337. [[CrossRef](#)]
16. Streubel, K.; Rapp, S.; André, J.; Chitica, N. 1.26 μm vertical cavity laser with two InP/air-gap reflectors. *Electron. Lett.* **1996**, *32*, 1369. [[CrossRef](#)]



© 2019 by the authors. Licensee MDPI, Basel, Switzerland. This article is an open access article distributed under the terms and conditions of the Creative Commons Attribution (CC BY) license (<http://creativecommons.org/licenses/by/4.0/>).